A Multiple-scale Study of Vegetative Response to Cockpit Karst Topography in Maolan, Guizhou, China, and Ciales, Puerto Rico, USA

Fuyuan Liang

Department of Earth, Atmospheric, and Geographic Information Sciences, Western Illinois University, Macomb, IL 61455, USA

Abstract: Literature in remote sensing shows that the study of the relationship between topography and vegetation is often conducted in large mountainous areas where topographic attributes vary significantly, and a multi-scale approach is applied in which the investigation gradually downscaled to coarser spatial resolutions. Little such research has been done in a typical cockpit karst area where the topographic properties usually don't exhibit significant variations and lower resolution data cannot be utilized for a small area like cockpit karst. This paper proposes an innovative approach to examine the correlations between topography and vegetation in a tropical (Ciales, Puerto Rico, USA) and a subtropical (Maolan, Guizhou, China) cockpit karst area. Topographic profiles were first constructed over individual karst residual hills at an azimuth increment of 22.5 degrees. The paired values of elevation and NDVI along the profiles were then extracted and correlation analysis were performed. The results indicate that significantly more profiles present high negative correlations between elevation and NDVI values, which could be attributed to the variations in moisture source resulting from the singular hydrogeological characteristics in cockpit karst areas. Slope aspect also shows its influences on vegetation. More south-facing profiles exhibit high negative correlations than north-facing profiles in the subtropical Maolan area. However, the difference is not statistically significant in the tropical Coals area, where variations in evapotranspiration between south-facing and north-facing slopes are not as significant as those in the subtropical karst areas.

Keywords: cockpit karst; topography; vegetation; NDVI; scale

---

1. Introduction

Literature in remote sensing shows that linkage between topography and vegetation growth condition is often conducted in mountainous areas, which presents significant variations in topographic attributes. The linkage is usually investigated at multi-scales by examining the correlation between topographic attributes and Normalized Difference Vegetation Index (NDVI) values, which were gradually downscaled to coarser spatial resolutions (e.g., [1,2]). To some extent, the downscaling process tends to disguise high frequency (local) variations in the topographic and NDVI data. It may not be an issue if the study is conducted in a

large area with significant variations in topographic and vegetation properties, such as the Santa Monica Mountains in California [2] and the Glacier National Park in Montana [1]. But this is not the case for typical cockpit karst areas, of which the topographic properties usually don't exhibit great variations. For example, the relief in cockpit karst in La Alinaza, Puerto Rico and Guilin, China is seldom more than 100 meters [3, 4]. Furthermore, the cockpit karst comprises residual hills surrounded by closed depressions, which are often smaller in size. In La Alinaz, PR, for instance, there are around 38 residual hills and 14 depressions per square kilometer [4]. It is obvious that high resolution digital elevation model (DEM) and remote sensing images are required to study the local variations in topographic and vegetative properties and any attempts to downscale the data would undermine, if not make it impossible, the linkage between topography and vegetation.

Cockpit karst topography consists of an array of star-shaped depressions surrounded by steep-sided residual hills and is mainly found in tropical and subtropical areas [2,5,6]. Immediately beneath the surface soil, carbonate in cockpit karst terrain is usually well weathered with plenty of solutionally enlarged joints, of which the extent and frequency diminish gradually with depth [7]. The zone of weathered carbonate (also known as epikarst or subcutaneous zone) is typically 3-10 m deep but could vary considerably in different places due to various lithology, structure, geomorphologic history and climate [7,8]. Karst landscapes are often waterless as surface water is drained vertically and quite rapidly through the enlarged joints at the depression bottoms. However, excessive water could be occasionally stored in the void spaces of the epikarst and a perched epikarst aquifer may temporally form when the rate of recharge exceeds the maximum rate of vertical throughput.

From the side slope to the depression center, the epikarst usually becomes thicker and contains more water because corrosion increases along the soil-rock interface next to the sink of a depression [9]. There is also a marked increase of soil thickness from the side slope to the bottom of the depression [9] due to a long-term balance between soil production and erosion. Soil in depression tends to have higher moisture content because of the centripetal flow of surface runoff and possible laminar subsurface flow owing to the negative topography. It is reasonable to expect increased water storage from the upper to lower slope due to the increased thickness of soil layer and the epikarst. Such a change in water storage amount should affect vegetation growth in cockpit karst areas. However, previous studies on cockpit karst mainly focus on their morphometric and hydrologic characteristics [8,10,11] and to our best knowledge no studies have been conducted to investigate the vegetative response to topography in cockpit karst areas.

In this paper, we present an innovative method to examine the correlations between topography and vegetation at a local scale along topographic profiles of two typical cockpit karst areas: Maolan, Guizhou, China and Ciales, Puerto Rico, USA, which fills the gap both in remote sensing and in cockpit karst study.

2. Study area

This study was conducted in two cockpit karst areas (Figure 1): one lies in the Maolan Natural Reserve (25.19°N, 107.91°E), Guizhou, China, and the other is in Ciales (18.34°N, 66.52°W), Puerto Rico. USA. The study area within the Maolan Natural Reserve has a humid subtropical monsoonal climate with mild temperature (the annual mean is 15°C) and plentiful precipitation (the annual mean is 1752 mm). The cockpit karst in this area is covered by evergreen broad-leaved mixed forest. Human intervention mainly occurs on the bottom of depressions, which is extensively cultivated. The forest on residual hills is mostly intact.

The residual karst hills in Ciales are developed under a tropical climate and is well blanketed with dense forest [12]. Although the forest is located within the moist forest life zone [12], it has a high proportion of deciduous tree species [13] and the stands tend to show signs of being exposed to frequent drought conditions. Human disturbance is barely noticed within the study area.

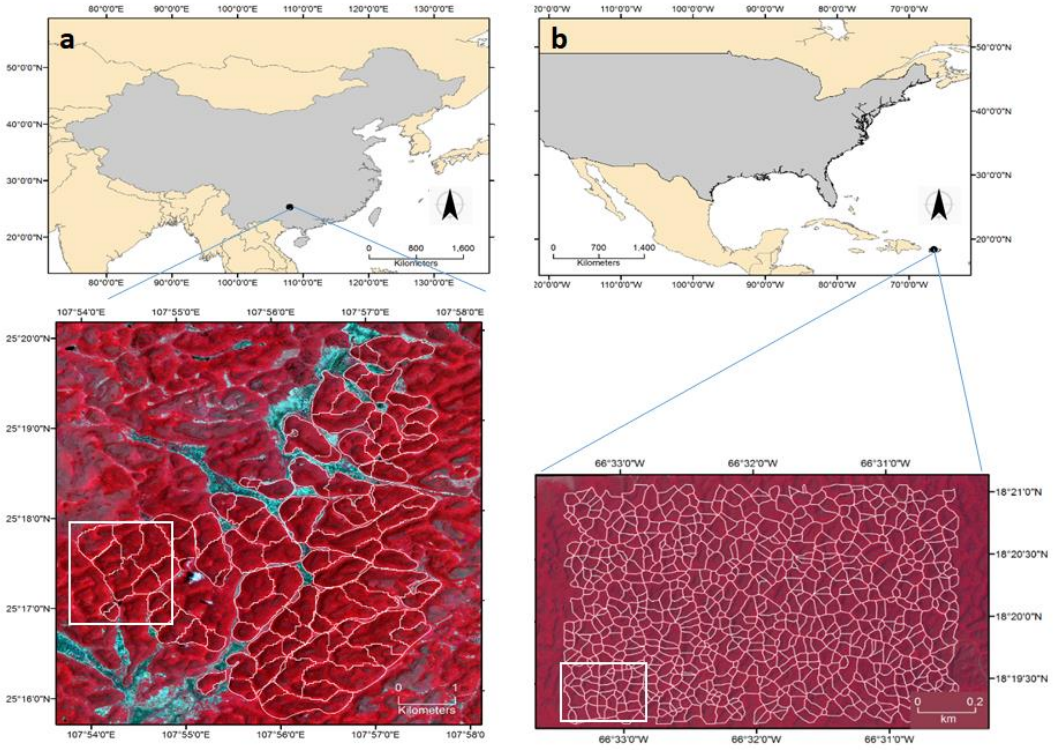

Figure 1 Maps of China and the USA showing the locations of the two study areas. The boundaries of the residual karst hills are shown in white thin line over the color-infrared displays of IKONOS and World View 03 images of Maolan and Ciales, respectively. The white rectangles on the images show the areal extent of the images in Figures 2A and 3A.

.

3. Materials and Methods

This study examined the variations in NDVI along topography profiles of karst hills in the two study areas to show how karst topography influences vegetation greenness. The whole process can be divided into the following three steps:

3.1 Delineation of karst hills and generation of topographic profiles

Digital elevation models (DEM) were used to delineate karst hills and construct topographic profiles. For Maolan study area, we adopted the ASTER global DEM, which has a spatial resolution of 30-m and is the best available DEM for this study area. For Ciales study area, the United States Geologic Survey (USGS) 10-m DEM was used to represent the topography.

To delineate karst hills, the DEM was first inverted and the hills in the original DEM thus were converted into depressions in the inverted DEM. The general watershed delineation GIS procedures were then performed to delineate each individual depression from the inverted DEM. Only the sinks with a depth less than 10 m and 3 m (1/3 of the spatial resolution of the DEMs) in Maolan and Ciales, respectively, were filled, as most sinks are natural features in karst areas [3]. The divides of the depressions were considered as the boundaries of the karst hills in the two study areas. The boundaries were further refined by visually checking the high resolution remote sensing images (explained in the sections to follow) to exclude the areas showing significant cultivation.

The topographic profiles were subsequently constructed over the surface of each karst hill. The highest point (the peak) in the original DEM was first identified for each hill, and 16 topographic profiles were subsequently constructed for each individual hill with an azimuth increment of 22.5 degrees starting from the right north (azimuth = 0) from its peak all the way down to its refined boundary.

3.2 Calculation of NDVI

Vegetation greenness is normally inferred from NDVI, which is calculated using the radiance data of the near infrared and red bands of remote sensing images [14,15] as in Equation (1):

$$NDVI = (NIR-R)/(NIR+R), \quad (1)$$

where NIR and R are the spectral radiance data recorded on the near infrared and red spectral bands of satellite remote sensing images, respectively. In this study, three images with different spatial resolutions were acquired for the Maolan study area, including an Ikonos image (4 m, acquired on 5/23/2004), an ASTER image (15 m, acquired on 11/22/2009), and a Landsat 7 image (30 m, acquired on 11/22/2009). For the Ciales study area, only a WorldView 03 image (2 m, acquired on 3/17/2011) and an ASTER image (15 m, acquired on 7/31/2015) were obtained for this study. No Landsat image was used for the Cailes area because the karst hills are small [4] and the 30-m spatial resolution Landsat image is not able to resolve the variations in vegetation greenness along the profiles. All images are orthorectified. Digital numbers of the pixels on each image were converted to top-of-atmosphere spectral radiance, which was used to calculate the NDVI.

3.3 Correlation analysis of elevation and NDVI along topographic profiles

Values of NDVI and elevation were first extracted from the NDVI and DEM datasets along each topographic profile at the same distance interval as the spatial resolution of the corresponding remote sensing image. In other words, the NDVI values derived from the WorldView 03, IKNOS, ASTER, and Landsat images were sampled along the topographic profiles every 2, 4, 15, and 30 meters, respectively. For a specific topographic profile, elevation values were also sampled at the same interval as the NDVI. Image analysis shows that the NDVI values are lower for the pixels in the topographic shadows than those fully illuminated. Therefore, this study excludes the profiles that are partially or entirely in topographic shadows and only examines those that are fully illuminated. The shadows in the images were delineated from the DEM-derived hillshades, which were produced using the hillshade function in ArcGIS. The azimuth angle and sun altitude of light source used to generate hillshade were exactly the same as when the remote sensing images were acquired.

Statistical analysis was then performed in SPSS to examine the correlations between the elevation and NDVI values along each topographic profile. The number and percentage of profiles were summarized based on the range of the correlation coefficient (r) value. In this study, we adopt the scheme proposed by [16] to determine the scale of correlation magnitude: high positive or negative correlation ($r>0.5$ or $r<-0.5$), low positive or negative correlation ($0.1\leq r<0.5$ or $-0.5\leq r<-0.1$), and trivial correlation ($-0.1<r<0.1$). The number and percentage of profiles were also summarized by the profile azimuth. We lastly applied the t statistical analysis to infer whether the influences of karst topography on vegetation greenness in the two study areas are statistically significant or not. All statistical analyses were conducted in SPSS.

4. Results

4.1 Topographic profiles

Figures 2(a) and 3(a) display the boundaries (enclosed thicker white lines) and topographic profiles (radiative thinner white lines) of a part of the residual hills in Maolan and Ciales, respectively. Scatterplots of NDVI and elevation values on exemplary profiles (1) and (2) (identified in Figures 2(a) and 3(a) demonstrate typical negative (Figures 2(b) and 3(b) and positive (Figures 2(c) and 3(c) correlations between NDVI and elevation in the two study areas.

In Ciales, 11,136 topographic profiles were constructed from the USGS DEM over the 696 karst hills (Table 1). We excluded 4,146 profiles that are horizontally shorter than 60 m to ensure that, in Ciales, at least four pairs of NDVI and elevation values could be extracted from the profile for correlation analysis at the scale of 15 m. There are, respectively, 0 and 2,215 profiles that are located in the topographic shadows on the WorldView 03 and the ASTER images in Ciales. In the end, we performed correlation analyses on 6,690 and 4,755 profiles on the WorldView 03 and ASTER images, respectively.

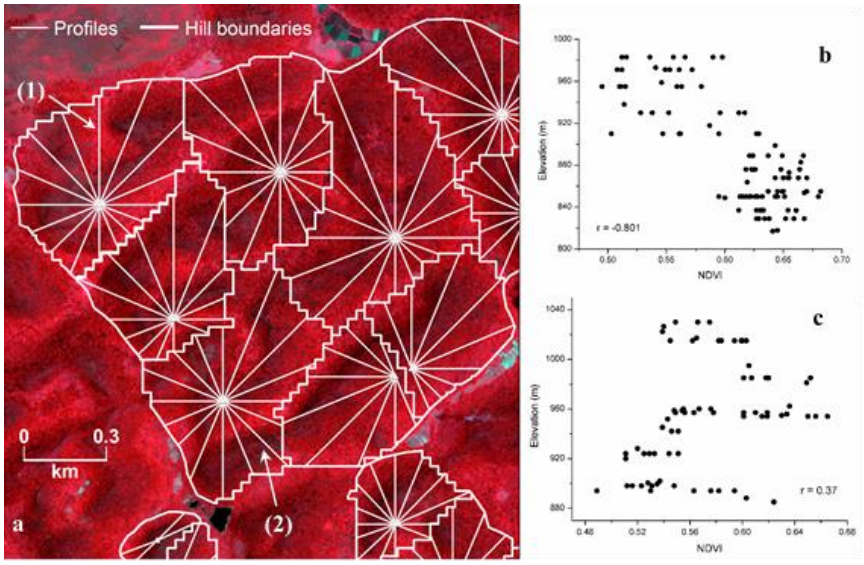

Figure 2. (a) Topographic profiles (radiative thin white lines) generated within a part of the residual hills in Maolan atop of the IKONOS image. Enclosed thicker white lines are boundaries of karst residual hills (b) Scatterplot of elevation and NDVI for exemplary profile (1) exhibiting a negative correlation; (c) Scatterplot of elevation and NDVI for exemplary profile (2) exhibiting a positive correlation.

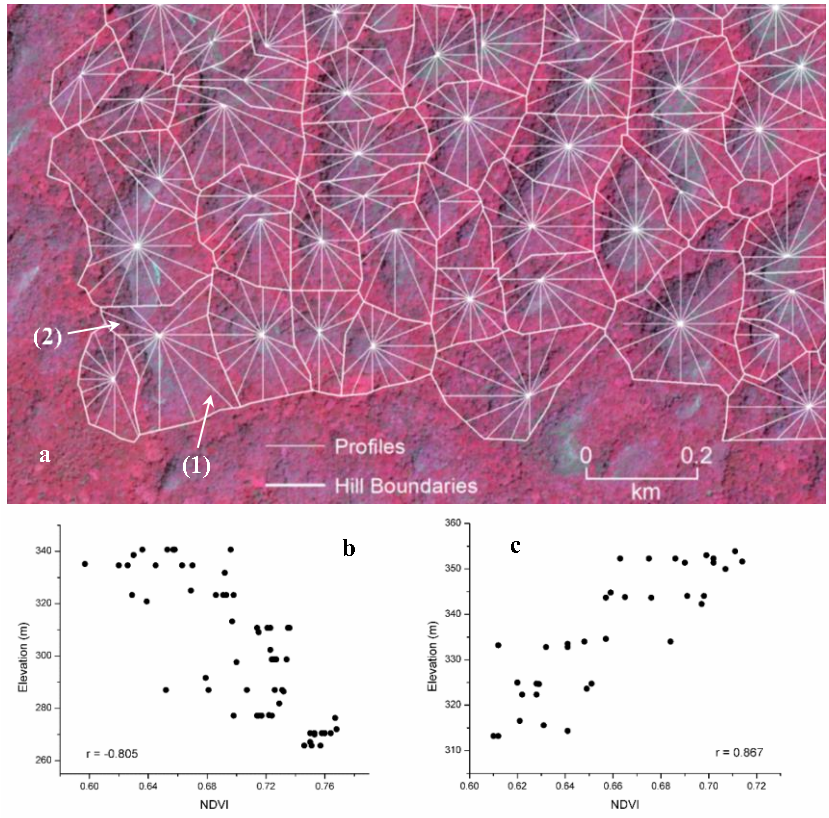

Figure 3. (a) Topographic profiles (radiative thin white lines) generated within a part of the residual hills in Ciale atop of the WorldView 03 image. Enclosed thicker white lines are boundaries of karst residual hills (b) Scatterplot of elevation and NDVI for exemplary profile (1) exhibiting a negative correlation; (c) Scatterplot of elevation and NDVI for exemplary profile (2) exhibiting a positive correlation.

205 Table 1. Statistics of topographic attributes and topographic profiles in the two study areas.
206

Statistics	Ciales, PR	Maolan, China
Elevation (m)	286.86 ± 41.35	877.71 ± 64.89
Slope gradient (°)	33.88 ± 12.9	29.57 ± 13.09
Total number of residual hills	696	98
Hill perimeter (m)	636.07 ± 193.01	2,319.12 ± 828.86
Hill planar size (km2)	0.024 ± 0.01	0.22 ± 0.12
Hill relief (m)	62.69 ± 26.21	188.81 ± 62.01
Total number of profiles generated	11,136	1,568
Number of profiles no less than 120 m	--	1,352
Number of profiles no less than 60 m	6,990	--
Profile length (m)	100.28 ± 35.23	257.75 ± 111.84
Profile slope gradient (°)	31.51 ± 7.93	26.38 ± 9.98

207

208 We constructed 1,568 profiles over the 96 karst residual hills in Maolan (Table 1)
209 and 209 of them were excluded from the analyses because they are shorter than 120
210 m, the minimum length to guarantee at least four pairs of NDVI and elevation
211 samples for each profile at the 30-m resolution. The numbers of profiles that are
212 fully illuminated on the 4-m IKONOS, 15-m ASTER, and 30-m Landsat images are
213 1,352, 1,016, and 979, respectively, due to the different sun azimuths and altitudes at
214 the time when the images were captured. Subsequently, correlation analyses were
215 conducted on these fully illuminated profiles.

216 *4.2 Magnitudes of correlations between NDVI and elevation*

217 Table 2 summarizes the percentages of profiles with different magnitudes of
218 correlations. Across the examined data scales, the vast majority of the profiles show
219 negative correlations (without considering the significance level) between NDVI
220 and elevation values in both study areas. The most prominent case is found in
221 Ciales at the scale of 15 m, where about 93% of the profiles present negative
222 correlations. Even in the least obvious case, at the 15-m scale in Maolan, 72% of the
223 profiles show negative correlations. In Ciales, 81.8% and 79.1% of the profiles
224 present statistically significant negative correlations at the scales of 2 m and 15 m,
225 respectively. In contrast, only 3% and 2% of the profiles show statistically
226 significant positive correlations. In Maolan, the percentages of profiles with
227 statistically significant negative correlations are 65.16%, 46.95%, and 42.69%,
228 respectively, at the scales of 4, 15, and 30 m, whereas only 9.91%, 9.75%, and 7.87%
229 profiles show statistically significant positive correlations at these scales. These
230 findings indicate the existence of an inverse relationship between NDVI and
231 elevation values in both study areas.

Table 2. Percentage of topographic profiles with different magnitudes of correlations at multiple scales in the two study areas. Numbers outside and inside the parentheses show percentages of profiles with statistically significant and insignificant correlations, respectively, at the confidence level of 0.95.

Study area – scale (m)	Fully illuminated profiles	High negative profiles (%)	Low negative profiles (%)	Trivial profiles (%)	Low positive profiles (%)	High positive profiles (%)
Ciales – 2	6,990	68.57 (0)	13.18 (7.35)	0 (4.76)	1.75 (3.12)	1.27 (0)
Ciales – 15	4,755	79.03 (9.25)	0.02 (5.24)	0 (1.24)	0 (2.00)	2.04 (1.18)
Maolan – 4	1,352	41.12 (0)	24.04 (11.61)	0 (8.80)	7.4 (4.51)	2.51 (0)
Maolan – 15	1,016	44.39 (2.66)	2.56 (20.57)	0 (6.59)	0.69 (12.11)	9.06 (1.38)
Maolan – 30	979	42.59 (10.52)	0.1 (16.04)	0 (7.05)	0 (10.73)	7.87 (5.11)

4.3 Variation of NDVI-elevation correlations with azimuths

Table 3 summarizes the percentages of the profiles with statistically significant negative correlations at each specific azimuth at different scales. Most profiles in Ciales present statistically significant negative correlations between NDVI and elevation in all azimuths, but there seems to be no consistent concentration of high-correlation profiles in any azimuth. In Maolan, contrastingly, south-facing profiles (with an azimuth closer to 180°) have significant negative correlations, especially when observed at 15 m and 30 m. Overall, fewer profiles have negative correlations in Maolan (averagely 49%) than Ciales (averagely 77%).

We further performed the paired samples t-test of the percentages of profiles with statistically significant high negative correlations to the total number of profiles at a specific azimuth to compare the difference in the percentage between the two areas at the same scale, as well as between different scales in the same area (Table 4). At the scale of 15 m for the two study areas, the difference of the average is statistically significant at the confidence level of 95% ($p= 0.000$). However, in the same study area, the difference of the average between multiple scales is not statistically significant at the significance level of 0.05 (Table 4).

Table 3. Percentages of topographic profiles with statistically significant (high and low combined) negative correlations between NDVI and elevation values at various azimuths at multiple scales. The azimuths were counted clockwise from north (0°).

Azimuth (°)	Ciales – 2 m	Ciales – 15 m	Maolan – 4 m	Maolan – 15 m	Maolan – 30 m
22.5	76.33	77.11	65.88	27.27	37.78
45.0	82.87	86.82	63.22	32.26	45.31
67.5	83.23	85.96	68.18	42.47	50.67
90.0	86.35	85.09	65.48	54.67	41.89
112.5	87.78	84.02	70.37	47.95	37.50
135.0	85.54	82.20	66.25	55.56	34.29
157.5	81.36	81.08	71.05	56.52	46.97
180.0	78.61	80.95	65.91	62.65	50.60
202.5	76.56	79.24	62.35	60.24	61.45
225.0	77.55	78.92	61.36	65.52	56.47
247.5	80.18	73.66	64.44	48.81	46.34
270.0	84.22	60.96	64.63	33.33	26.98
292.5	83.94	58.72	69.05	33.33	7.69
315.0	82.88	43.08	57.14	18.75	12.00
337.5	79.72	49.41	64.77	23.33	34.62
360.0	80.49	64.20	63.41	20.69	37.04
Average	81.73	73.21	65.22	42.71	39.23

Table 4. Paired samples t-test of the percentages of profiles with statistically significant high negative correlations to the total number of profiles.

		Paired Differences			t-test		
Areas	Scale pair (m)	Mean	Std. Deviation	Std. Error Mean	t	df	Sig.(2-tailed)
Between areas	15 vs. 15	32.811	12.577	3.144	10.435	15	0.000
Ciales	2 vs. 15	-4.649	13.416	3.354	-1.386	15	0.186
Maolan	4 vs. 15	0.746	11.936	2.984	0.250	15	0.806
	4 vs. 30	2.009	12.604	3.151	0.637	15	0.533
	15 vs. 30	1.263	13.181	3.295	0.383	15	0.707

At each individual scale, we grouped the profiles into the south- and north-facing groups based on their azimuths. The south-facing group includes all profiles with an azimuth of 135°, 157.5°, 180°, 202.5° and 225°, and the north-facing group consists of profiles with an azimuth of 315°, 337.5°, 360°, 22.5° and 45°. We then performed paired sample t-tests to evaluate the differences between the two

groups (Table 5). In Ciales, the mean differences of the percentages in the south- and north-facing groups (south minus north) are 1.64 and 16.35 at the scale of 2 m and 15 m, respectively. The difference is not statistically significant at the confidence level of 95% (p = 0.427 and 0.136, respectively). In Maolan, the mean differences of the percentages in the south- and north-facing groups (south minus north) are 8.46, 35.29, and 16.61 at the scales of 4, 15, and 30 m, respectively. All these differences are statistically significant at the significance level of 0.05 (p = 0.016, 0.00, and 0.003, respectively). The above results indicate that in Maolan, more south-facing profiles tend to show negative correlations between NDVI and elevation than north-facing profiles. In contrast, no significant differences exist between south- and north-facing profiles in Ciales.

Table 5. Paired sample *t*-tests of differences between south-facing and north-facing profiles in terms of percentage of profiles with statistically significant high negative NDVI-elevation correlations.

Study area	Scale (m)	South mean	North mean	Paired difference (south – north)			*t*	*p* (2-tailed)
				Mean	Standard deviation	Standard error mean		
Ciales	2	67.22	65.58	1.64	4.15	1.86	0.883	0.427
	15	80.48	64.12	16.35	19.64	8.78	1.862	0.136
Maolan	4	44.32	35.86	8.46	4.68	2.09	4.037	0.016
	15	57.42	22.13	35.29	3.6	1.61	21.891	0
	30	49.96	33.35	16.61	5.9	2.64	6.293	0.003

5. Discussion

NDVI, a function of the red and near-infrared spectral radiance recorded by remote sensors, is widely used for examining vegetation greenness. The red band radiance is inversely proportional to the amount of chlorophyll existed in the plant canopy, whereas the near-infrared band radiance is positively related to green or photosynthetically active vegetation [15]. A higher NDVI value normally suggests a denser green leaf cover, thus more greenness, whereas a lower NDVI value indicates less greenness. Decline in NDVI, thus greenness, is of great significance as it may indicate the loss of photosynthetic capacity of vegetation, which, if presents at a large areal extent, may suggest a significant perturbation to the global carbon cycle [17,18].

Variations in NDVI and greenness usually show alteration of leafy vegetation dynamics. At a continental or regional scale, significant drop in NDVI tends to reflect major disturbances in vegetation. Water stress may be the most frequent events of disturbance. For example, Xu et al. [15] examined the variations in NDVI from images obtained by the Moderate Resolution Imaging Spectroradiometer (MODIS) and identified a widespread decline in greenness of vegetation in Amazon region due to the strong drought in 2010. Variations in NDVI are also found strongly related to drought conditions over grasslands in the central Great Plains of

the United States [19]. Changes in NDVI can even document regional vegetation die-off as a result of severe droughts [20].

Results presented in this study reveal that water stress also has impacts on vegetation greenness at a local scale. As listed in Table 3, the majority of the topographic profiles show negative correlations between elevation and NDVI values, i.e., less greenness at the upper slope and more greenness at the lower slope. In other words, there tends to be sparser green leaf cover at the upper slope but denser cover at the lower slope along the profiles. This trend of decrease in NDVI from the lower slope to the upper slope could be mainly attributed to water stress in the two study areas, as other stresses such as insect outbreak, wild fire, or anomaly lower temperature were not reported in the two study areas during the period of interest. Lugo et al. [12] argued that the forest in Ciales is located within a moisture life zone with an annual precipitation of 1659 mm, but forest stands exhibit signs of being exposed to frequent drought conditions. It seems that the forest stands in cockpit karst areas tend to be frequently affected by short spells of droughts, though no similar studies are conducted in Maolan area, where the annual precipitation is in the same magnitude of Ciales.

Water stress in forest stands in cockpit karst areas is essentially associated with the hydrological characteristics of cockpit karst. Most cockpit karst areas are characterized by a thin layer of soil overtop the significantly weathered carbonate rocks. Vertical openings are ubiquitous in tropical and subtropical karst areas due to extensive subsurface chemical weathering. Even there is plenty of precipitation in the two study areas, surface water often disappears quickly through the extensive subsurface openings. Moreover, limited amount of soil water can be retained in the thin soil layer. Thus, forest stands in cockpit karst areas tend to show signs of being exposed to frequent droughts, which usually develop when water in soil evaportranspirates and or water in the epikarst aquifer (which occasionally develops after heavy rain) drains out.

The negative correlations between NDVI and elevation values along the topographic profiles indicate that forest stands at the upper slope are more vulnerable to water stress than those at the lower slope. This can be explained by the increased thickness of soil layer (thus increased soil water), the increased thickness of the epikarst (thus more water could be temporally stored in the epikarst aquifer), and a gradual decline in groundwater depth from the upper to the lower slope [7,21]. The characteristic hydrological settings of cockpit karst provide forest stands at the lower slope of the profiles more access to moisture and therefore lead to denser leaf cover and higher NDVI values. By contrast, forest stands at the upper slope are more vulnerable to more frequent droughts due to limited access to soil, epikarst aquifer, and ground water, and thus have sparser leaf cover and lower NDVI values.

Denser leaf cover at the lower slope and sparser leaf cover at the upper slope are more evident along the profiles facing south. In both of the two study areas, higher proportion of the south-facing profiles present high negative correlations than that of the profiles facing north (Table 5). The difference could be attributed to

the stronger evapotranspiration on the south-facing slopes, which receive higher solar insolation than the north-facing slopes. However, the difference is statistically significant in the subtropical Maolan study areas at 4-m, 15-m, and 30-m scales but not significant in the tropical Ciales study area at either 2-m scale or 15-m scale. This suggests that the difference of evapotranspiration between south-facing and north-facing slopes in the tropical Ciales is not as significant as that in the subtropical Maolan area. The possible reason for the significant difference in evapotranspiration between south- and north-facing slopes in Maolan area is that there is significant difference in total annual solar radiation between south- and north-facing slopes in higher latitude areas (Maolan) than that in lower latitude area (Ciales) [22].

In the same area, there is no statistically significant difference in the proportion of profiles with statistically significant high negative correlations at a specific azimuth between multiple scales (Table 4). In Ciale, the difference at scales of 2 m and 15 m is -4.65% and is not statistically significant at the confidence level of 95% ($p= 0.186$). In Maolan area, none of the differences between scales of 4 m, 15 m, and 30 m is statistically significant at the confidence level of 95%. This suggests that the influence of topography on vegetation greenness is evident, no matter at what scales the correlations are examined. The scale-independent negative correlation also suggests a promising future to examine the temporal variation of correlations between NDVI and vegetation greenness by using multi-temporal and multi-scale remote sensing images. This is extremely important to study disturbance events (such as drought, wild fire, and insect break) of vegetation, particularly in tropical and subtropical area, where cloud is usually an obstacle for the same remote sensing system to acquire images within a short revisit time period.

6 Conclusions

This study examined the multi-scale topological influences on vegetation greenness in two cockpit karst areas, which are characterized by residual hills surrounded by closed depressions. We first constructed radiating profiles from the peak to the foothill of each karst residual hill at an azimuth increment of 22.5 degrees. Along the profiles, elevations were derived from DEMs and the index of vegetation greenness (NDVI) was obtained from remote sensing images with different spatial resolutions. Correlation analysis was then performed and percentage of profiles showing negative and positive correlations in different magnitudes was summarized to investigate the relationship between elevation and NDVI values along the profiles.

Significantly more profiles show statistically significant negative correlations between elevation and NDVI values along the profiles in the two cockpit karst areas, suggesting denser leaf cover (more greenness) at the lower slope and sparser leaf cover (less greenness) at the upper slope of the topographic profiles. The increasing greenness from the upper slope to the lower slope reflects that the forest stands at the upper slope are exposed to more frequent water stress conditions than those at the lower slope. The variations of exposure to water stress could be

explained by the singular hydrogeological characteristics in cockpit karst areas. The bottom of the depression tends to have a shallow and groundwater table, a thick layer of soil, and a thicker epikarst aquifer (though temporary), which all provide more moisture to the forest stands there. By contrast, limited moisture sources are available to the forest stands growing at the upper slope due to a deeper groundwater table, a very thin soil layer, and a thinner epikarst aquifer.

Topographic influences on vegetation greenness is not significant at different scales. The influences are more evident when the slope aspects are further considered. More south-facing profiles show negative correlations between elevation and NDVI values than north-facing profiles in both of the two study areas. This could be attributed to the stronger evapotranspiration in the south-facing slopes than that in the north-facing slopes. However, the difference of the percentages in south- and north-facing profiles is statistically significant in the subtropical Maolan area but not statistically significant in the tropical Ciales area. It is reasonable as the difference of solar radiation received by the north- and south-facing slopes is much more significant in higher latitude area than lower latitude area. Such a difference, combined with the singular hydrogeological characteristics of karst depression, controls the varied moisture availability at the upper slope and the lower slope, and therefore the variations in vegetation greenness along the topographic profiles.

References

1. Bian, L.; Walsh, S.J. Scale Dependencies of Vegetation and Topography in a Mountainous Environment of Montana. *Prof Geogr.* **1993**, *45*, 1–11.
2. Deng, Y.; Chen, X.; Chuvieco, E.; Warner, T.; Wilson, P. Multi-Scale Linkages between Topographic Attributes and Vegetation Indices in a Mountainous Landscape. *Remote Sens. Environ.* **2007**,*111*, 122–134, DOI:10.1016/j.rse.2007.03.016.
3. Liang, F.; Xu, B. Discrimination of Tower-, Cockpit-, and Non-Karst Landforms in Guilin, Southern China, Based on Morphometric Characteristics. *Geomorphology* **2014**, *204*, 42–48, DOI:10.1016/j.geomorph.2013.07.026.
4. Liang, F.; Du, Y.; Ge, Y.; Li, C. A Quantitative Morphometric Comparison of Cockpit and Doline Karst Landforms. *J. Geogr. Sci.* **2014**, *24*, 1069–1082, DOI:10.1007/s11442-014-1139-6.
5. Day, M.J.; Huang, W. Reflections on Fengcong and Fenglin. J. *Cave and Karst Science* **2009,** *36*, 49–51.
6. Lyew-Ayee, P.; Viles, H. A.; Tucker, G.E. The Use of GIS-Based Digital Morphometric Techniques in the Study of Cockpit Karst. *Earth Surf. Process. Landf.* **2007**, *32*, 165–179, DOI:10.1002/esp.1399.
7. Ford, D. C.; Williams, P. *Karst Hydrogeology and Geomorphology*; Wiley, Chichester, 2007, ISBN: 9780470849965.
8. Williams, P.W. The Role of the Epikarst in Karst and Cave Hydrogeology: A Review. *Int J Speleol* **2008**, *37*, 1-10.

9. Zambo, L.; Ford,D.C. Limestone Dissolution Processes in Beke Doline Aggtelek National Park, Hungary. *Earth Surf. Process. Landf.* **1997**, *22*, 531–543.
10. Williams, P.W. Morphometric Analysis of Polygonal Karst in New Guinea. *Geol Soc Am Bull.* **1972**, *83*, 761-796.
11. Williams, P.W. The Role of the Subcutaneous Zone in Karst Hydrology. *J. Hydrol.* **1983**, *61*, 45–67.
12. Lugo, A.E.; Castro, L.M.; Vale, A.; López, T.M.; Prieto, E.H.; Martinó, A.G.; Alberto, R.; Rolón, P. Puerto Rican Karst-a Vital Resource. 2004. General Technical Report-USDA Forest Service, no. WO-65. http://www.cabdirect.org/abstracts/20073247785.html.
13. Chinea-Rivera, J.D. The Forest Vegetation of the Limestone Hills of Northern Puerto Rico, Cornell University, New York, USA, Aug. 1980.
14. Rouse Jr, J.W.; Haas, R.H.; Schell, J.A.; Deering, D.W. Monitoring Vegetation Systems in the Great Plains with ERTS. *NASA Special Publication* **1974,** *351*, 309-317.
15. Tucker, C. J. Red and Photographic Infrared Linear Combinations for Monitoring Vegetation. *Remote Sens. Environ.* **1979**, *8*,127–150.
16. Cohen, J. *Statistical power analysis for the behavioral sciences*, 2nd ed.; Hillsdale, NJ: Erlbaum, 1988. ISBN: 9780805802832.
17. Potter, C.; Kumar, V.; Klooster, S.; Nemani, R. Recent History of Trends in Vegetation Greenness and Large-Scale Ecosystem Disturbances in Eurasia. *Tellus B* **2007**, *59*, 260–272, DOI:10.1111/j.1600-0889.2006.00245.x.
18. Xu, L.; Samanta, A.; Costa, M.H.; Ganguly, S,; Nemani, R.R.; Myneni, R.B. Widespread Decline in Greenness of Amazonian Vegetation due to the 2010 Drought. *Geophys. Res. Lett.* **2011**, *38*, L07402, DOI:10.1029/2011GL046824.
19. Gu, Y.; Brown, J.F.; Verdin, J.P.; Wardlow, B. A Five-Year Analysis of MODIS NDVI and NDWI for Grassland Drought Assessment over the Central Great Plains of the United States. *Geophys. Res. Lett.* **2007**, 34, L06407, DOI:10.1029/2006GL029127.
20. Breshears, D.D.; Cobb, N.S.; Rich, P.M.; Price, K.P.; Allen, C.D.; Balice, R.G.; Romme, W.H.; Kastens, J.H.; Floyd, M.L.; Belnap, J.; Anderson, J.J.; Myers, O.B.; Meyer, C.W. Regional Vegetation Die-off in Response to Global-Change-Type Drought. *Proceedings of the National Academy of Sciences of the United States of America* **2005**, *102*, 15144–15148.
21. Williams, P. ed. *Karst Terrains: Environmental Changes and Human Impact. Catena Supplement.* Vol. 25. Catena Verlag. 1993. ISBN: 3923381344.
22. Kondratyev, K.Y.; Fedorova, M.P.; Radiation regime of inclined surfaces, *Solar Energy* **1977**, *1*, 36–61.